Pure & Appl. Chem., Vol. 69, No. 11, pp. 2263–2269, 1997.
Printed in Great Britain.

High-temperature heat-capacity measurement up to 1500 K by the triple-cell DSC

Yoichi Takahashi

Department of Applied Chemistry, Chuo University, Bunkyo-ku, Tokyo 112, Japan

Abstract: Although precise heat-capacity data at high temperatures are very important for modern technology such as nuclear engineering, space technology etc, the reliable methods of measurements up to 1000℃ are scarce. We developed a new differential scanning calorimeter (DSC) for heat-capacity measurements from room temperature to 1500 K. In order to overcome difficulties encountered in high-temperature heat-capacity measurements with conventional DSC equipment, two new concepts were adopted for the design of this apparatus: a "triple-cell" system and triple-adiabatic temperature control. The heat capacities of several metals were determined from 300 to 1500 K to test the new apparatus. The heat capacities of Ni and Ti, which are known to have phase transitions were also successfully measured. The precision of the apparatus was estimated to be within ±3%. Some experimental results on important nuclear fuels are also given.

INTRODUCTION

Needs for heat-capacity data at high temperatures above 1000 K are increasing in such fields as nuclear engineering, space technology, energy storage systems, etc. Measurements of heat capacity at such high temperatures have been performed mainly drop calorimetry, in which, however, heat capacity cannot be measured directly, thus a certain arbitrariness in the determination becomes unavoidable.

Differential scanning calorimetry (DSC) has been used to study the thermal behavior of materials and to determine their heat capacities. The temperature range of the heat capacity measurements, however, has as far been usually limited to below 1000 K. The main reason for this limitation is ascribed to the fact that radiation heat-loss increases with temperature and, as a result, the thermal stability and repeatability of the isothermal baseline signals become poor. For precise heat-capacity measurements at high temperatures, it is thus necessary to stabilize the temperature control and establish the isothermal baseline.

In order to overcome the difficulties encountered at high temperatures with conventional DSC, we adopted two new concepts for the design of a new DSC; a "triple-cell" system(1) and triple adiabatic temperature control, and successfully developed(2) a new DSC system for precise heat-capacity measurements up to 1500 K, as described below.

THE NEW DSC APPARATUS

The principle of the triple-cell DSC

In order to realize precise heat-capacity measurements at high temperatures, we adopted the new "triple-cell" concept, first described by Wunderlich(1). The principle of the triple-cell system is shown in Fig. 1 in comparison with conventional one. The sample section of this apparatus consists of three identical sites for sample cells; a cell with sample to be measured, a cell with reference material, and an empty cell. The temperature differences between the sample and the empty cells (ΔT_s) , and between the reference and the empty (ΔT_r) cells are detected by R-type thermocouples under a constant heating rate. The heat capacity of the sample is calculated by comparing these two signals. This measuring system eliminates the necessity of three separate runs as must be done in a conventional twin-cell system. Once the calibration constant is determined as the difference of sensitivity between the sample side and the reference side, the heat capacity is determined by only two separate runs including a blank (all-empty -cells) run. Thus, the heat capacity of the sample, C_s, can be obtained by

$$C_s = C_r \cdot \frac{R_r}{R_s} \cdot \frac{\Delta T_s - (\Delta T_s)_{blank}}{\Delta T_r - (\Delta T_r)_{blank}}, \quad (1)$$

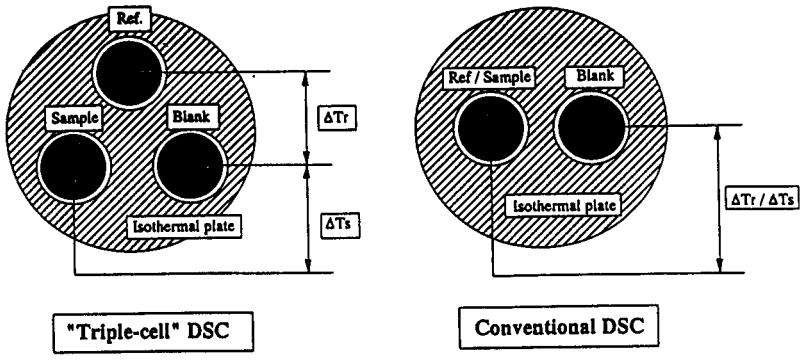

Fig. 1 Conceptual diagram of the triple-cell DSC in comparison with the conventional twin-cell system.

where C_r is the heat capacity of the reference material, R_s and R_r the thermal resistance of the sample side and that of the reference side, respectively, and (R_r / R_s) gives the calibration constant, k.

Experimental set-up of the apparatus

Sample section and cells. Schematic diagrams of the sample section are shown in Fig. 2. The top view shows the location of the cells for the sample, the reference and the empty sides. Each cell has a sample-pan holder, made of Pt-13%Rh flat plates 0.3mm thick, which is connected by three bridges (0.3mm in width) to the isothermal plate, in order to avoid the effect of cross-flow between the cells and to provide adequate thermal resistance for detection. The isothermal plate is made of Pt-13%Rh alloy, and is set in an isothermal container made of Pt-10%Rh alloy.

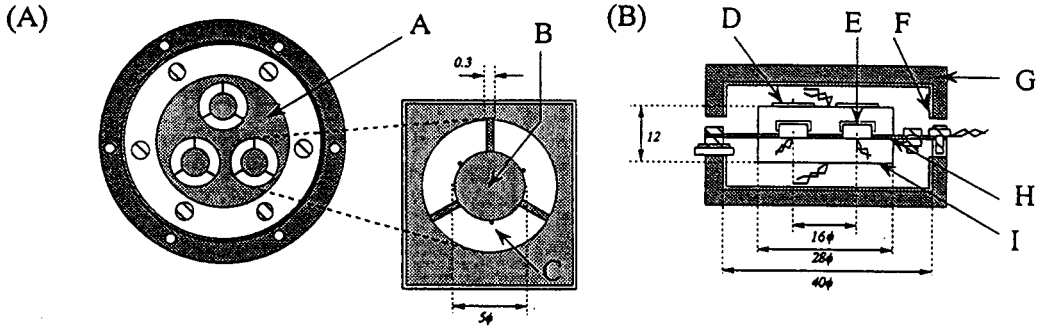

Fig. 2 Schematics of the sample section. A, isothermal plate; B, sample holder; C, pin for holding sample cell; D, lid; E, sample cell; F, platinum foil; G, adiabatic wall; H, isothermal plate; I, isothermal container.

Adiabatic control. When measuring precise heat capacities at high temperatures, sufficient temperature control is most important. We therefore adopted the triple-adiabatic temperature control system to attain thermal stability in the calorimeter. The sample section is surrounded by three adiabatic walls. Platinum foils are put inside the walls in order to minimize radiation heat-loss. The innermost adiabatic wall is divided into upper and lower sections, each of which can be controlled separately to eliminate the effect of convection of inert gas. They are further surrounded by double adiabatic walls, and the thermal stability is secured by all of these adiabatic walls. It is considered that the temperature fluctuations in the sample section are within about ±0.1 K during measurement.

Temperature sensing system. A block diagram of the temperature sensing system is shown in Fig. 3. R-type thermocouples, 0.3mm in diameter, are used for detecting temperature differences. The Pt-wires are connected to the rear surface of the sample holders of the three cells, and the isothermal plate made of Pt-13%Rh alloy acts as another contact for the wires of the thermocouples. The output signals of temperature differences between the empty side and the reference side and between the empty side and the sample side, are detected by these thermocouples with the Pt-wire connected to the sample side and a Pt-13%Rh wire connected to the center of the isothermal plate. The thermocouple for measuring the sample temperature was calibrated using pure metals (Sn, Ag).

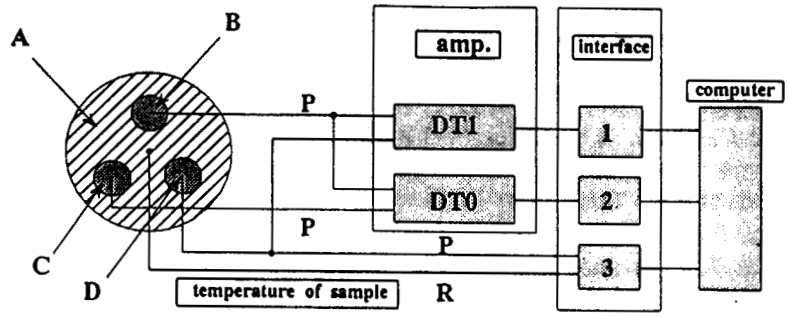

Fig. 3 Block diagram of the temperature-sensing system. A, isothermal plate; B, empty side; C, reference side; D, sample side.

Analytical procedure

For heat capacity measurements, two different methods, a scanning method and an enthalpy method, have been used. The "scanning method" refers to heat capacity measurements in which the output signals are continuously converted to heat capacity values over the range of the temperature scan. The procedure is schematically shown in Fig. 4. On the other hand, in the "enthalpy method", all the output signals during a temperature scan are integrated to give the total enthalpy change (ΔH) for the given temperature interval (ΔT). The quantity $\Delta H / \Delta T$ is taken as the value of the heat capacity at the midpoint of the temperature interval. The sequence of enthalpy runs is shown schematically in Fig. 5.

RESULTS OF HEAT CAPACITY MEASUREMENTS

Determination of the calibration constant

The apparatus was calibrated, prior to the measurements, using the NBS reference material α-Al_2O_3(SRM-720). In the calibration, the enthalpy method was used, in which the total enthalpy change of

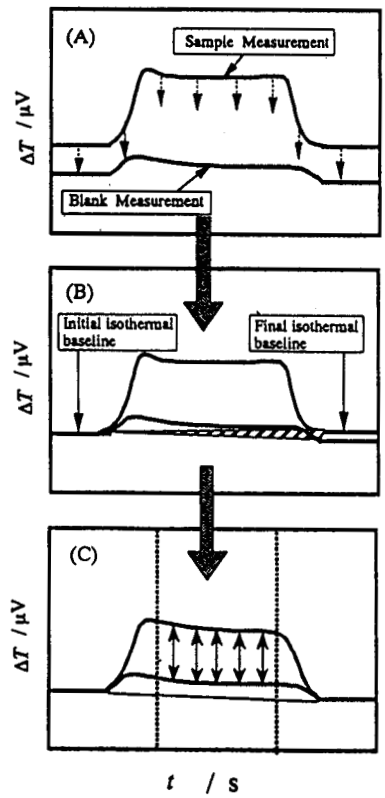

Fig. 4 Schematic of the procedure for the scanning method.

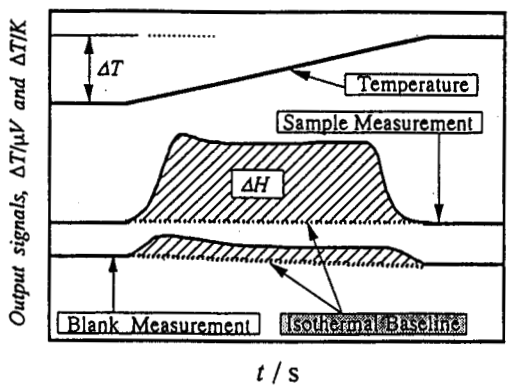

Fig. 5 Schematic of the procedure for the enthalpy method.

the sample over a 25 K interval was measured with a scanning rate of 5 K min^{-1}. In order to check the difference in sensitivity between the sample side and the reference side, two pieces of the α-Al_2O_3 samples were placed on the sample side and the reference side, with the empty pan on the empty side, and the calibration constant ($k=R_r/R_s$) was determined over the range from 300 to 1500 K. The results are shown in Fig. 6. It can be seen that the calibration constant is roughly equal to unity below 1000 K, but it deviates slowly from unity above 1000 K with increasing temperature. This may be attributed to the change in heat transfer from conduction through the isothermal plate to radiation. The experimental uncertainty of this apparatus was considered to be within ±1-2% below 1000 K, and ±2-3% above this temperature.

Heat capacity of metals

Platinum and molybdenum. The heat capacity of Pt was determined using the enthalpy method from 300 to 1500 K. The results are shown in Fig. 7, together with the literature values(3, 4). The two series of experimental results are consistent within the estimated experimental uncertainty, by about 1%. The reproducibility of the data was considered to be ±2-3% over the temperature range of the measurements.
The heat capacity of Mo determined from 300 to 1500 K is also consistent with the literature values(5), within the estimated experimental uncertainty, indicating the high reliability of the new DSC apparatus.

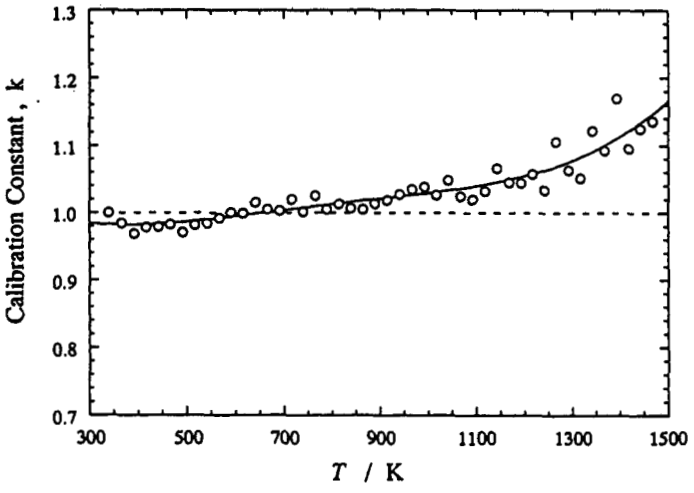

Fig. 6 Calibration constant k for heat-capacity measurements. ○, experimental values; ——, polynomial expression.

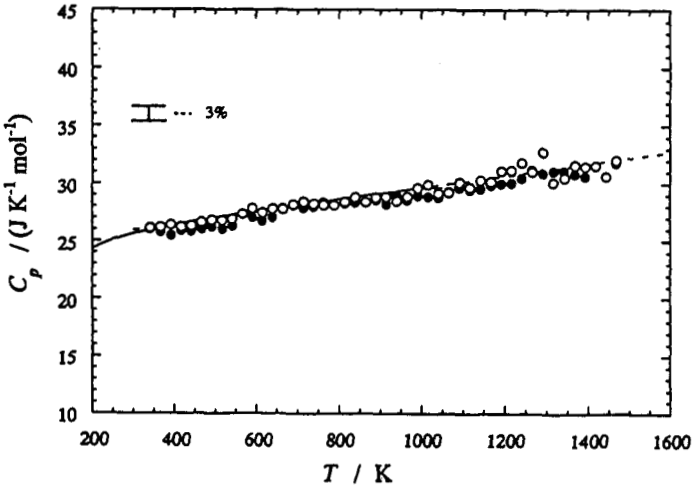

Fig. 7 Heat capacity of Pt. ○, ●, runs 1 and 2(present work); – – –, Hultgren et al. (3); ——, Yokokawa and Takahashi (4).

Nickel and titanium : the application to the heat-capacity anomaly. Heat-capacity measurements were also carried out on Ni and Ti, which are examples of materials having thermal anomalies. Nickel shows a heat-capacity anomaly caused by a magnetic transition at 631 K. The results obtained for Ni by the enthalpy method are shown in Fig. 8(a). Measurements were carried out four times on several samples of different thicknesses. The four series of data are consistent with each other within ±3%, and also agree well with the literature values(6-8), although out data are slightly lower. Thus, even around a thermal anomaly, the heat capacity can be determined with a precision of ±3% using this DSC apparatus.

The heat-capacity measurements were also carried out by the scanning method, with a long scan over the 473-673 K temperature range. The results are shown in Fig. 8(b). The scanning method has the advantage in determining the transition temperature more exactly than the enthalpy method. The transition temperature observed in this study was 629 K.

Titanium is also known to have a thermal anomaly caused by a structural phase transition at around 1160 K. The observed heat-capacity values by the enthalpy method are shown in Fig. 9(a). A sharp peak at around 1160 K was observed. Below the transition temperature, the present data are lower by 3-7% than the literature values(9,10). This discrepancy may be the effect of some impurities, such as dissolved oxygen. The purities of the samples used in the literature were reported to be 98.7-99.7%, less than that of the sample used here (≥99.9%). Dissolved oxygen in metals has been known to increase the heat capacity(11). Furthermore, the transition peaks reported in the literature(12) were considerably broader than that of the present result, indicating some effect of impurities. We believe that our heat-capacity values are reasonable in

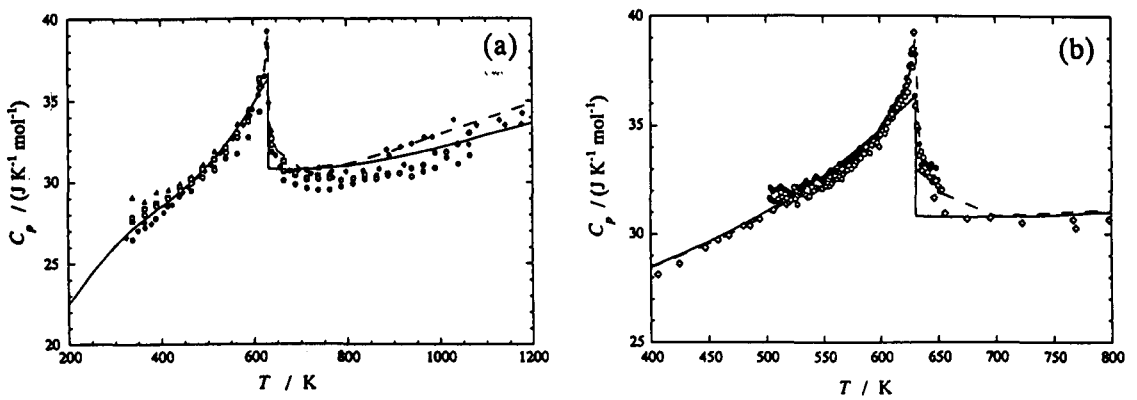

Fig. 8 (a) Heat capacity of Ni by the enthalpy method. △, □, ○, ●, runs 1, 2, 3 and 4 (present work); ——, JANAF data (6); ◇, TPRC data (7); – – –, Hultgren et al. (8). (b) Heat capacity of Ni by the scanning method. ●, ○, runs 1 and 2 (present work); ——, JANAF data (6); ◇, TPRC data (7); – – –, Hultgren et al. (8).

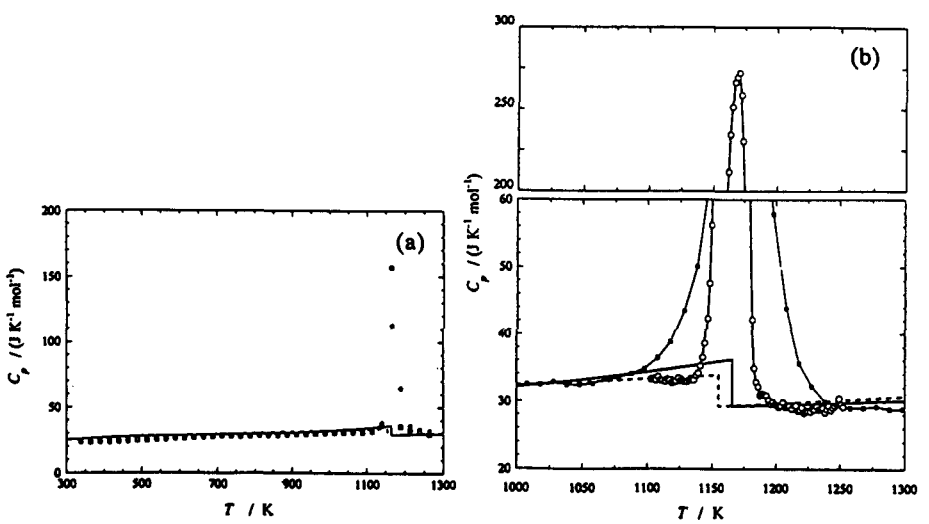

Fig. 9 (a) Heat capacity of Ti by the enthalpy method. □, ●, runs 1 and 2 (present work); ——, JANAF data (9); – – –, Hultgren et al.(10). (b) Heat capacity of Ti by the scanning method.○, present work; ——, JANAF data (9); – – –, Hultgren et al. (10); ■, Backhurst (12).

this respect. Measurements by the scanning method with a long scan over the 1073-1273 K temperature range showed a sharp peak as shown in Fig. 9(b). The observed transition temperature, which was determined by extrapolating the leading edge of the peak to the baseline, was 1148 K. Although this value is slightly lower than the literature values (1155-1160 K), this disagreement must also be attributable to oxygen impurities in the samples, as can be seen from the phase diagram of the Ti-O system(13).

Nuclear applications : Heat capacity of UO_2 and $(U,Gd)O_2$(14)

High-temperature heat capacity of $(U,Gd)O_2$ has been paid attentions because it is one of the most important properties for the design of nuclear fuel assemblies. Figure 10 shows the results of heat-capacity measurements on UO_2 and $U_{0.858}Gd_{0.142}O_2$ from 300 to 1500 K. The results on UO_2 agree well with the literature values(15), although our values are slightly lower, by about 2%. The reproducibility of the values was ±2-3% over the temperature range of the measurements. This indicates that the heat capacity can be determined precisely (±2-3%) up to 1500 K, even for a sample of low thermal conductivity.
The heat capacity values for the mixed oxide have almost similar temperature dependence to those of pure UO_2 up to 1500 K. It should be noted that we observed no thermal anomaly over the temperature region investigated, in contrast to the reported results of Inaba et al.(16). Our results are supported by the recent report of the measurements on SIMFUEL(17).

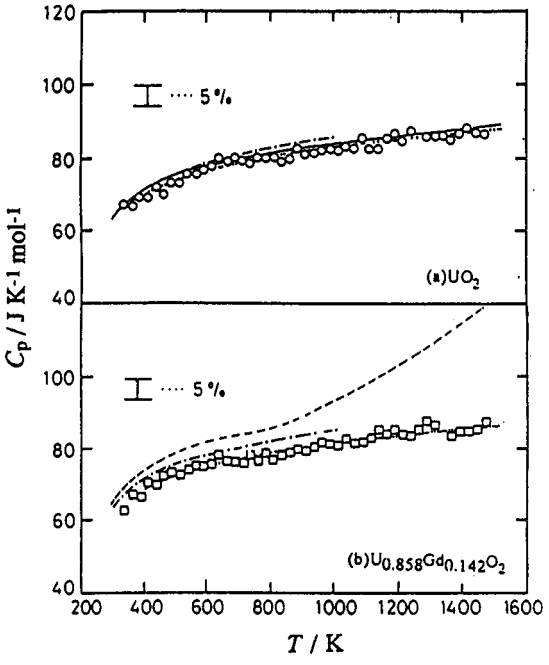

Fig. 10 Heat capacities of (a) UO_2 and (b) $U_{0.858}Gd_{0.142}O_2$ determined by DSC. ○, □ and - • • - , present work and its smoothed curve; • - - - •, Takahashi and Asou(14); — — —, Inaba et al. on $U_{0.858}Gd_{0.142}O_2$ (16); ——, Fredrickson et al. on UO_2(15).

CONCLUSION

A new differential scanning calorimeter (DSC) for heat-capacity measurements up to 1500 K has been developed, using a "triple-cell" system and a "triple-adiabatic" temperature control system. The heat capacities of several metals such as Pt, Mo, Ni and Ti were determined from 300 to 1500 K, and the precision of the heat capacity measurements was estimated to be within ±3%. Using the scanning method, it was possible to determine the profile of heat-capacity anomalies. The heat capacities of UO_2 and gadorinia-doped UO_2 were also determined, and no significant thermal anomaly was observed on $(U, Gd)O_2$ up to 1500 K.

ACKNOWLEDGMENTS

The author is deeply indebted to Drs. M. Asou, M. Kamimoto and A. Maesono for their collaboration throughout this work.

REFERENCES

1. B. Wunderlich. *J. Therm. Anal.* **32**, 1949 (1987).
2. Y. Takahashi and M. Asou. *Thermochim.* Acta **223**, 7 (1993).

3. R. Hultgren, P. D. Desai, D. T. Hawkins, M. Gleiser, K. K. Kelley and D. D. Wagman. *Selected Values of the Thermodynamic Properties of the Elements*, p. 396. Am. Soc. for Metals, Metals Park, OH (1973).
4. H. Yokokawa and Y. Takahashi. *J. Chem. Thermodyn.* **11**, 411 (1979).
5. D. A. Ditmars, A. Cezairliyan and T. B. Douglas. *NBS Special Publication, No. 260*, p. 55. (1970).
6. *JANAF Thermochemical Tables*, 3rd edn., p. 1621. ACS/AIP/NBS (1985).
7. Y. S. Touloukian and E. H. Buyco. *Thermophysical Properties of Matter, Specific Heat; Metallic Elements and Alloys*, P.146. IFI/Plenum, New York (1970).
8. R. Hultgren, P. D. Desai, D. T. Hawkins, M. Gleiser, K. K. Kelley and D. D. Wagman. *Selected Values of the Thermodynamic Properties of the Elements*, p. 350, Am. Soc. for Metals, Metals Park, OH (1973).
9. *JANAF Thermochemical Tables*, 3rd edn., p. 1818. ACS/AIP/NBS (1985).
10. R. Hultgren, P. D. Desai, D. T. Hawkins, M. Gleiser, K. K. Kelley and D. D. Wagman. *Selected Values of the Thermodynamic Properties of the Elements*, p. 516. Am. Soc. for Metals, Metals park, OH (1973).
11. J. Nakamura, Y. Takahashi, S. Izumi and M. Kanno. *J. Nucl. Mater.* **88**, 64 (1980).
12. I. Backhurst. *J. Iron Steel Inst. (London)*, **189**, 124 (1958).
13. J. L. Murray and H. A. Wriedt. *Bulletin of Alloy Phase Diagrams*, **8**(2), 148 (1987).
14. Y. Takahashi and M. Asou. *J. Nucl. Mater.* **201**, 108 (1993).
15. D. R. Fredrickson and M. G. Chasanov. *J. Chem. Thermodyn.* **12**, 623 (1970).
16. H. Inaba, K. Naito and M. Oguma. *J. Nucl. Mater.* **149**, 341 (1987).
17. R. A. Verrall and P. G. Lucuta. *J. Nucl. Mater.* **228**, 251 (1996).